Lowest $^1\Sigma_g$ and $^1\Sigma_u$ states of the hydrogen molecule in strong magnetic fields: An application of the configuration-interaction method with Hylleraas-Gaussian basis set

Xuanyu Song,[1,2] Haoxue Qiao,[1] and Xiaofeng Wang[1,*]
[1]*Department of Physics, Wuhan University, Wuhan 430072, China*
[2]*College of Physics and Electronic Engineering, Xinyang Normal University, Xinyang 46400, China*
(Received 28 March 2012; published 1 August 2012)

With the Hylleraas-Gaussian basis set, in which the term of r_{12}^1 is expanded approximately in Gaussian-type geminals, a full configuration-interaction (CI) method is applied to calculate the lowest $^1\Sigma_g$ and $^1\Sigma_u$ states of the hydrogen molecule in magnetic fields up to 2.35×10^7 T. In the absence of magnetic field, the total energies of the lowest $^1\Sigma_g$ and $^1\Sigma_u$ states in our calculation are $-1.174\,447\,7(4)$ at the equilibrium distance of $R = 1.40$ a.u and $-0.756\,613\,4(6)$ at $R = 2.43$ a.u., respectively. Compared to the CI method with Gaussian basis set, a significant improvement in the precision of the total energies and the dissociation energies at corresponding equilibrium distances has been achieved. The z_1-z_2 probability density distributions in different field regions are calculated and analyzed.

DOI: 10.1103/PhysRevA.86.022502 PACS number(s): 33.15.−e, 32.60.+i, 95.30.Ky

I. INTRODUCTION

Since the discovery of huge magnetic fields of 10^2–10^5 T in white dwarfs [1] and 10^7–10^9 T in neutron stars [2], the electronic structure of atomic and molecular systems in strong magnetic fields has become a very interesting subject for several decades [3]. The strong magnetic effects also exist in semiconductors with small effective electron mass and large dielectric constants. For example, the unit of strong magnetic field is $H_{\rm eff}^0 = m_{\rm eff}^2 e^3 c/\varepsilon^2\hbar^3$ for the hydrogenlike excitons in direct-gap semiconductors, which is 6.57 T in CaAs [3] and could be less than 1 T in Ge and InSb [4].

Most of the investigations are focused on simple atomic systems in strong magnetic fields. Now we have abundant knowledge concerning the behaviors of hydrogenlike and heliumlike atoms in strong magnetic fields [5–10]. A full configuration-interaction (CI) method with an anisotropic Gaussian basis set was performed for the helium atom in the field region of 0–100 a.u. (1 a.u. corresponds to 2.35×10^5 T) [11,12]. Total energies for spin singlet and triplet states with positive and negative z parity in the subspace of magnetic quantum number $M = 0$ and $M = -1$ have been provided. However, the calculations of triplet states were easier than that of singlet states, because the cusp at the origin and the strong electronic correlation between the two electrons for singlet states is difficult to treat with the superposition of Gaussians. To overcome the disadvantage of the Gaussian basis set, a kind of Hylleraas-Gaussian basis set including r_{12}^1 and $r_{12}^{1/2}$ was applied to calculate the ground and low-lying states of the helium atom in strong magnetic fields [13]. The ground state of the helium atom is improved to $-2.903\,715$, which is much better than $-2.903\,351$ obtained by Becken *et al*. using a Gaussian basis set [11], and the accuracy of the calculation increases with increasing field strength.

Compared to many investigations about atoms in strong magnetic fields, the studies of molecular systems are rarely reported. As the simplest molecular system, the hydrogen molecular ion H_2^+ was investigated in many references [14–23]. Some valuable information on general magnetic-field-induced properties of molecular systems can be extracted from the study of the H_2^+ ion. With the Born-Oppenheimer approximation, the validity of which in the presence of strong magnetic fields has been studied by Schmelcher *et al*. [20], Guan *et al*. investigated the H_2^+ ion in an aligned strong magnetic field by a generalized pseudospectral method [21]; accurate data on equilibrium distances, binding energies, and dissociation energies for the ground and low-lying states were obtained. Highly precise results of the H_2^+ ion in a strong magnetic field were obtained by Vincke *et al*. and Baye *et al*. using the Lagrange-mesh method for parallel to the molecule axis [22] and arbitrary orientations [23]. In Ref. [24], Turbiner and López-Vieyra presented a detailed review of the qualitative and quantitative works about the one-electron molecular systems H_2^+, H_3^{2+}, H_4^{3+}, $(HeH)^{2+}$, and He_2^{3+} in a magnetic field ranging from 10^5 T to 4.414×10^9 T.

There would be more phenomena and behaviors for multielectron molecular systems in strong magnetic fields due to the correlation between electrons. However, even for the simplest multielectron molecular system, there exist only a few studies about the electron structure and properties of the hydrogen molecule in strong magnetic fields [25–35]. With a basis set of nonorthogonal, nonspherical Gaussian orbitals and the CI method, Detmer *et al*. performed a detailed investigation on the total energies, dissociation energies, and potential curves of the $^1\Sigma_g$, $^1\Sigma_u$, $^3\Sigma_g$, $^3\Sigma_u$, $^1\Pi_g$, $^1\Pi_u$, $^3\Pi_g$, and $^3\Pi_u$ states of the hydrogen molecule in magnetic fields [33,34]. It was found that, for the hydrogen molecule oriented parallel to the magnetic field, the ground state is the $^1\Sigma_g$ state for $\gamma \leqslant 0.18$ a.u., and it changes to the unbound $^3\Sigma_u$ state for $0.18 \leqslant \gamma \leqslant 12.3$ a.u. For strong magnetic fields of $\gamma \geqslant 12.3$ a.u., the ground state is the strongly bound $^3\Pi_u$ state. More recently, the variations in electron density and bonding for the lowest $^1\Sigma_g$ state of the hydrogen molecule under strong magnetic fields have been investigated by a time-dependent density functional theory [35]. However, the result of the ground state $^1\Sigma_g$ in the field-free case is higher than that

*Author to whom correspondence should be addressed: tulatin_wang@whu.edu.cn

obtained by Detmer. In this work, we apply the CI method based on the Hylleraas-Gaussian basis set, which has been successfully applied to the two-electron atomic system [13], to the calculation of the hydrogen molecule in magnetic fields.

II. THEORY AND METHOD

The hydrogen molecule is treated by the Born-Oppenheimer approximation. The origin of coordinates coincides with the middle point of the internuclear axis of the hydrogen molecule and the nuclei are located on the z axis. Assuming that the direction of the magnetic field is parallel to the molecule axis and a symmetric gauge for the vector potential of the magnetic field is used, the nonrelativistic Hamiltonian of the hydrogen molecule in a magnetic field reads in atomic units

$$H = \sum_{i=1}^{2}\left\{\frac{1}{2}\left(\boldsymbol{P}_i+\frac{1}{2}\boldsymbol{B}\times\boldsymbol{r}_i\right)^2-\frac{1}{|\boldsymbol{r}_i-\boldsymbol{R}/2|}-\frac{1}{|\boldsymbol{r}_i+\boldsymbol{R}/2|}\right\} -\frac{1}{r_{12}}+\frac{1}{R}+\boldsymbol{B}\cdot\boldsymbol{S}, \tag{1}$$

where $\boldsymbol{R}$ and R are the vector and magnitude of the internulcear distance, r_{12} is the distance between the two electrons, and $\boldsymbol{B}$ and $\boldsymbol{S}$ are the vectors of magnetic field and total electronic spin, respectively. The field strength is measured by the parameter $\gamma = B/B_0$ with $B_0 = 2.35 \times 10^5$ T. The upper bounds to the energies of the hydrogen molecule in magnetic fields are obtained by solving the Schrödinger equation using the Rayleigh-Ritz variational method.

The trial wave function of the Hamiltonian in Eq. (1) is written as a product of the spatial and the spin part, i.e.,$\Psi_{\rm tot} = \Psi\chi$. Using the linear combination of atomic orbitals–molecular orbitals (LCAO-MO) ansatz, Ψ can be written as

$$\Psi = \sum_{ij} c_{ij} r_{12}^n \left[\Phi_i^P(\boldsymbol{r}_1)\Phi_j^P(\boldsymbol{r}_2) \pm \Phi_i^P(\boldsymbol{r}_2)\Phi_j^P(\boldsymbol{r}_1)\right], \quad n = 0,\ 1, \tag{2}$$

where Φ_i^P and Φ_j^P are one-electron molecular orbitals of the H_2^+ ion. The molecular orbitals are built from atomic orbitals centered at each nucleus, which have been established in Ref. [16]:

$$\Phi_i^P(\boldsymbol{r}) = \phi_i\left(\boldsymbol{r}, +\frac{R}{2}\right) + (-1)^{P+P_a}\phi_i\left(\boldsymbol{r}, -\frac{R}{2}\right), \tag{3}$$

$$\Phi_j^P(\boldsymbol{r}) = \phi_j\left(\boldsymbol{r}, +\frac{R}{2}\right) + (-1)^{P+P_a+P_g}\phi_j\left(\boldsymbol{r}, -\frac{R}{2}\right). \tag{4}$$

P and P_a are the parities of the H_2^+ ion and corresponding atomic orbitals while P_g is the parity of the hydrogen molecule. The $\phi_i[\boldsymbol{r}, \pm(R/2)]$ and $\phi_j[\boldsymbol{r}, \pm(R/2)]$ are the atomic orbitals centered at the nuclei, which have the forms

$$\phi_i\left(\boldsymbol{r}, +\frac{R}{2}\right) = \rho^{|m_i|+2k_i}\left(z-\frac{R}{2}\right)^{l_i} e^{-\alpha_i\rho^2-\beta_i[z-(R/2)]^2} e^{im_i\varphi}, \tag{5}$$

and

$$\phi_i\left(r, -\frac{R}{2}\right) = \rho^{|m_i|+2k_i}\left(z+\frac{R}{2}\right)^{l_i} e^{-\alpha_i\rho^2-\beta_i[z+(R/2)]^2} e^{im_i\varphi}, \quad \text{with } m_i = \ldots -2, 0, 1, 2, \ldots,\ L_i = 0, 1, 2\ldots. \tag{6}$$

Here α_i and β_i are positive nonlinear variational parameters. To obtain these parameters, the standard simplex method [36] has been applied in the one-particle optimization procedure of the H_2^+ ion and H atom. We also use a direct two-particle optimization procedure of the hydrogen molecule.

The advantage of our basis set is the Hylleraas term r_{12}^1, which is used to describe the correlation between electrons. The key step is that r_{12}^1 is replaced by an approximate expansion of Gaussian-type geminals:

$$r_{12}^1 \approx \sum_\nu b_\nu\left(1-e^{-\tau_\nu r_{12}^2}\right). \tag{7}$$

The integrals of all the matrix elements can be evaluated in Cartesian coordinates (see the Appendix for a detailed example).

III. RESULTS AND DISCUSSIONS

Let us discuss the strategy for the selection of the basis functions first. As the projection L_z of the electronic angular momentum commutes with the Hamiltonian in Eq. (1), the angular momentum numbers m_i and m_j of the two molecular orbitals must satisfy the constraints $m_i + m_j = M$. Here we take the selection of the basis functions of the lowest $^1\Sigma_g$ state at field strength $\gamma = 1.0$ a.u. for an example. We select 32 H_2^+ molecular orbitals Φ_i optimized for $m_i = 0$ (17 with gerade parity $P = 0$ and 15 with ungerade parity $P = 1$), and we select 35 hydrogen atomic orbitals optimized for $m_j = 0$ to constitute the molecular orbitals Φ_j (18 with $P = 0$ and 17 with $P = 1$). Then the molecular orbitals Φ_i and Φ_j, combined with the Hylleraas term r_{12}^n, compose 561 basis functions according to Eq. (2). It is useful to choose the molecular orbitals with opposite angular momentum numbers ±1, and ±2 or higher to combine a total angular momentum $M = 0$, and the procedure is similar to that of $m_i = 0$ and $m_j = 0$. In the final trial wave function, we also include about 1200 H_2 molecular orbitals attained by direct two-particle optimization, combined with the Hylleraas term as well. The combination strategy in this work could be demonstrated as $\{\alpha_i^{H_2^+}, \beta_i^{H_2^+}, \alpha_j^H, \beta_j^H, r_{12}^0\}$ and $\{\alpha_i^{H_2}, \beta_i^{H_2}, \alpha_j^{H_2}, \beta_j^{H_2}, r_{12}^{0/1}\}$. Considering the size of the basis set and the computational time, only the two-particle optimized parameters $\{\alpha_i^{H_2}, \beta_i^{H_2}, \alpha_j^{H_2}, \beta_j^{H_2}\}$ are combined with r_{12}^1.

Table I presents the convergence of the total energy with including more configurations, as well as the contributions to the total energy from different configurations for the lowest $^1\Sigma_g$ state at the equilibrium distance $R = 1.23$ a.u. at the field strength $\gamma = 1.0$ a.u. The quantity R_c in the last column shows the ratio of successive difference defined in Ref. [37] and $E_t(\infty)$ is the extrapolated energy using the last $R_c = 3.72$. The different sign of ΔE is due largely to the Hylleraas term r_{12}^n, which leads to a mixture of configurations. The absolute value of contribution decreases with increasing m_i. As the contribution of $(+4, -4)$ configuration is about 10^{-7} order of magnitude, the configurations with m_i greater than 3 are

TABLE I. Total energies and the contributions (in atomic units) from different configurations for the hydrogen molecule of the lowest $^1\Sigma_g$ state at the field strength $\gamma = 1.0$ a.u. E_t stands for the total energy using the configuration and all configurations listed before it. R_c and E_t (∞) are the convergence ratio and the extrapolated energy, respectively.

(m_i, m_j)	Number of terms	ΔE	E_t	R_c
(0, 0)	1464	− 1.733 838 967 6	− 0.891 101 505	
(+1, −1)	2347	0.029 413 416 4	−0.891 175 345	
(+2, −2)	2775	0.000 228 775 4	−0.891 180 110	15.49
(+3, −3)	3175	0.000 005 444 3	−0.891 182 241	2.23
(+4, −4)	3575	0.000 000 387 6	−0.891 182 813	3.72
$1/R$		0.813 008 130 0		
γS_z		0.000 000 000 0		
Total	3575	−0.891 182 813 9		
E_t (∞)			−0.891 183 1(3)	

excluded in our calculation, and we limit k_i in Eqs. (5) and (6) to 0 and l_i to 0 and 1 for the same reason. The final sizes of our basis sets are about 2100–3200 for the lowest $^1\Sigma_g$ state and about 1500–2500 for the lowest $^1\Sigma_u$ state, respectively.

Table II lists the equilibrium distances R_{eq}, the dissociation energies E_d, and the total energies E_t at the equilibrium distances for the lowest $^1\Sigma_g$ state in magnetic fields. The blanks in the equilibrium distances column mean that they are equal to the equilibrium distance calculated by the Hylleraas-Gaussian basis set. Most results of the equilibrium distance for the lowest $^1\Sigma_g$ state are in good agreement with that obtained by Detmer *et al.* [33] from the field-free case to $\gamma =$ 100 a.u. Only for the case of $\gamma = 0.1$ a.u. and $\gamma = 1.0$ a.u., the equilibrium distances calculated with Hylleraas-Gaussian basis set are 1.40 and 1.23 a.u., respectively, while they are 1.39 and 1.24 a.u. in Ref. [33]. The total energy at the equilibrium distance $R = 1.40$ a.u. in the field-free case is −1.174 447 7(4) in our calculation. Compared to −1.173 892 obtained by the full CI method [33] with a large Gaussian basis set, our result has an improvement of about 5×10^{-4} a.u. and is much closer to −1.174 475 931 400 216 7(3) at the equilibrium $R = 1.4011$ a.u. obtained by Pachucki [38]. The Hylleraas-Gaussian basis set provides a better description of the real wave function, so that the results are improved about 5×10^{-4} a.u. on average in the presence of magnetic fields. While increasing the field strength, the equilibrium distance R_{eq} decreases and the corresponding dissociation energy increases monotonously.

Figure 1 shows the energy curve of the lowest $^1\Sigma_g$ state for specific field strengths, where the energy of the vertical axis is shown with respect to the dissociation limit, i.e., $E(R) = E_t(R) - \lim_{R\to\infty} E_t(R)$. It is shown clearly that the equilibrium distance decreases, while the depth of the well increases dramatically with increasing field strength. The dissociation energy at the equilibrium distance increases with increasing field strength (inset of Fig. 1).

For the lowest $^1\Sigma_u$ state in the field-free case, the equilibrium distance and the total energy at the equilibrium distance, 2.43 and −0.756 690 483, respectively, were obtained with high accuracy by Cencek *et al.* [39]. The corresponding data amount to 2.42 a.u. and −0.756 111, respectively, in Ref. [33] using a Gaussian basis set. Our results obtained by the Hylleraas-Gaussian basis set are 2.43 a.u. and −0.756 613 4(6), respectively, which are in good agreement with Cencek's accuracy results. In Table III, most equilibrium

TABLE II. Equilibrium distances R_{eq}, total energies E_t, and dissociation energies E_d at equilibrium distances of hydrogen molecule for the lowest $^1\Sigma_g$ state as a function of field strengths γ. All quantities are in atomic unit.

γ	R_{eq}	R_{eq}[a]	E_d	E_t	E_t[a]	$\lim_{R\to\infty} E_t$
0.0	1.40		0.174 447 8(4)	− 1.174 447 7(4)	− 1.173 436[b] − 1.173 892[c]	− 0.999 999 9
0.01	1.40		0.174 459 7(4)	− 1.174 409 6(4)	− 1.173 396	− 0.999 949 9
0.05	1.40		0.174 743 7(4)	− 1.173 497 0(4)	− 1.172 407	− 0.998 753 3
0.1	1.40	1.39	0.175 608 8(4)	− 1.170 661 7(4)	− 1.169 652	− 0.995 052 9
0.2	1.39		0.178 816 0(4)	− 1.159 579 0(4)	− 1.158 766	− 0.980 763 0
0.5	1.33		0.195 329(2)	− 1.089 750(2)	− 1.089 082	− 0.894 421 0
1.0	1.23	1.24	0.228 846(2)	− 0.891 184(2)	− 0.890 336	− 0.662 337 7
2.0	1.09		0.291 808(2)	− 0.336 236(2)	− 0.335 574	− 0.044 427 7
5.0	0.86		0.438 714 0(5)	1.800 488 3(5)	1.801 212	2.239 202 3
10.0	0.70		0.616 163 8(1)	5.888 242 2(1)	5.889 023	6.504 406 0
50.0	0.417		1.372 545(2)	42.591 739(2)	42.592 815	43.964 284 0
100.0	0.334		1.914 328 8(3)	90.506 070 3(3)	90.506 974	92.420 399 1

[a]Reference [33].
[b]Larger basis set.
[c]Smaller basis set.

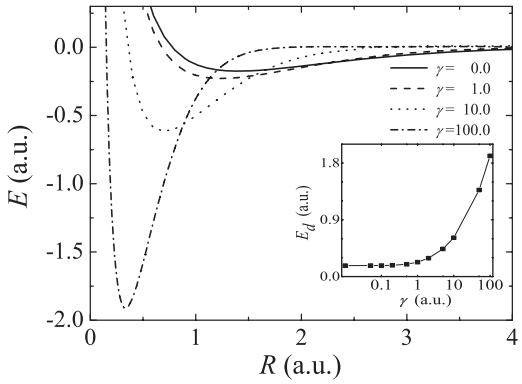

FIG. 1. Potential-energy curves (PECs) of the lowest $^1\Sigma_g$ state for $\gamma = 0.0$, 1.0, 10.0, and 100.0 a.u. The quantity of the vertical axis is taken as $E(R) = E_t(R) - \lim_{R\to\infty} E_t(R)$. The inset shows the evolution of the dissociation energies at the equilibrium distances with increasing field strength.

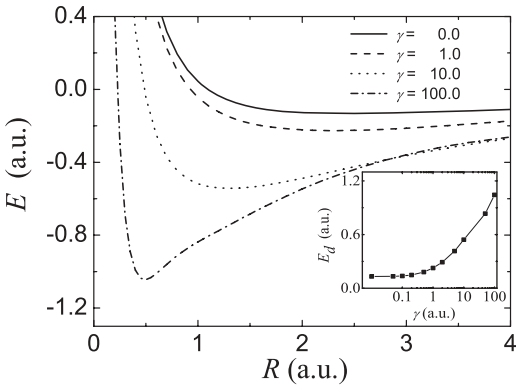

FIG. 2. PECs of the lowest $^1\Sigma_u$ state for $\gamma = 0.0$, 1.0, 10.0, and 100.0 a.u. The quantity of the vertical axis is taken as $E(R) = E_t(R) - \lim_{R\to\infty} E_t(R)$. The inset shows the evolution of the dissociation energies at the equilibrium distances with increasing field strength.

distances are in good agreement with the results obtained by Detmer except for $\gamma \leqslant 0.1$ a.u. For $\gamma \leqslant 0.1$ a.u. our equilibrium distances are larger than that obtained through Gaussian basis by 0.01 a.u. Compared with the energies calculated with the Gaussian basis set, an improvement of about 5×10^{-4} a.u. is obtained from $\gamma = 0.01$ to 50 a.u. With increasing magnetic field strength the dissociation channel of the lowest $^1\Sigma_u$ state changes from $H(0^+) + H(0^-)$ to $H_2 \rightarrow H^-(0_s^+) + H^+$ (the subscript s denotes that the H^- state is a singlet state) at about $\gamma \sim 20$ a.u. So the calculated total energies of the H^- for corresponding states at the field strength of $\gamma = 50$ and 100 a.u. are provided in the last column in Table III, while they are 46.359 385 and 95.436 219, respectively, in Ref. [40]. We also plot the energy curve of the lowest $^1\Sigma_u$ state for specific field strengths in Fig. 2. The quantity of the vertical axis in Fig. 2 is the same as that of Fig. 1 and the inset shows the evolution of the dissociation energy at the equilibrium distance with increasing field strength. It shows that the equilibrium distance decreases and the depth of the well increases with increasing field strength.

Figure 3 shows the z_1-z_2 probability density distribution of the hydrogen molecule for the lowest $^1\Sigma_g$ state at the corresponding equilibrium distance. It is mainly distributed in the second and the fourth quadrants, which indicates that the two electrons tend to reside in the vicinity of a different nucleus. With increasing the field strength, the z_1-z_2 probability density distribution of the lowest $^1\Sigma_g$ state at the equilibrium distance is compressed to the vicinity of the origin, which leads to a higher probability of electrons locating between the two nuclei so that the Coulomb repulsion between two nuclei is reduced. As a direct consequence, the equilibrium distance between the nuclei decreases and a larger binding energy is induced.

Figure 4 shows a different distribution pattern of the probability density for the $^1\Sigma_u$ state, where the probability is large in the first and third quadrants. The coordinates of the largest probability density shown by the white cross in Fig. 4(a) are $z_1 = -1.2$ a.u. and $z_2 = -1.2$ a.u. (or $z_1 = 1.2$ a.u, $z_2 = 1.2$ a.u.) at $\gamma = 0$ a.u. and $R = 2.42$ a.u., which means that the electrons tend to locate near the same nucleus and in a plane vertical to the z axis. The point with the largest probability density is also shown at $\gamma = 100$ a.u and $R = 0.490$ a.u. in Fig. 4(d) by the white cross with $z_1 = -0.2$ a.u. and $z_2 = -0.5$ a.u. [or the other three points where (z_1, z_2)

TABLE III. Equilibrium distances R_{eq}, total energies E_t, and dissociation energies E_d at equilibrium distances of hydrogen molecule for the lowest $^1\Sigma_u$ state as a function of field strengths γ. All quantities are in atomic unit.

γ	R_{eq}	R_{eq}[a]	E_d	E_t	E_t[a]	$\lim_{R\to\infty} E_t$
0.0	2.43	2.42	0.131 613 5(6)	− 0.756 613 4(6)	− 0.756 111	− 0.624 999 9
0.01	2.43	2.42	0.131 685 1(6)	− 0.756 510 4(6)	− 0.756 069	− 0.624 825 3
0.05	2.44	2.43	0.133 260 4(6)	− 0.754 101 9(6)	− 0.753 408	− 0.620 841 5
0.1	2.47	2.46	0.137 199 5(5)	− 0.747 136 0(5)	− 0.746 347	− 0.609 936 5
0.2	2.53		0.147 787 3(5)	− 0.723 352 8(5)	− 0.722 812	− 0.575 565 5
0.5	2.50		0.181 091 3(5)	− 0.603 062 1(5)	− 0.602 596	− 0.421 970 8
1.0	2.30		0.226 133 1(9)	− 0.317 308 5(9)	− 0.316 748	− 0.091 175 4
2.0	2.01		0.291 483 7(6)	0.388 591 4(6)	0.389 051	0.680 075 1
5.0	1.60		0.415 427 6(3)	2.856 555 8(3)	2.857 162	3.271 983 4
10.0	1.30		0.543 099 9(3)	7.326 453 3(3)	7.327 008	7.869 553 2
50.0	0.667	0.666	0.834 437 0(4)	45.524 424 2(2)	45.524 983	46.358 861 2(2)
100.0	0.490		1.044 165 5(2)	94.391 042 2(1)	94.391 271	95.435 207 7(1)

[a]Reference [33].

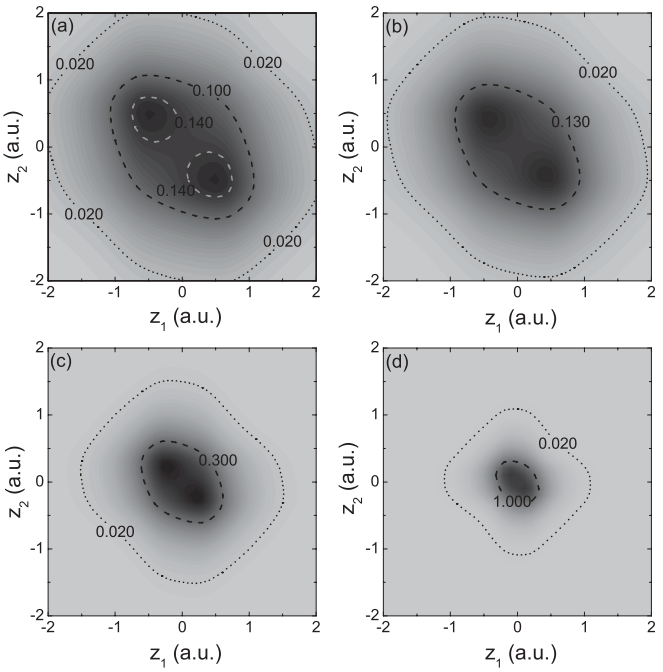

FIG. 3. The z_1-z_2 probability density distribution of the lowest $^1\Sigma_g$ state at equilibrium distance for specific field strength. (a) $\gamma = 0.0$ a.u., $R = 1.4$ a.u.; (b) $\gamma = 1.0$ a.u., $R = 1.23$ a.u.; (c) $\gamma = 10.0$ a.u., $R = 0.70$ a.u.; (d) $\gamma = 100.0$ a.u., $R = 0.334$ a.u. The length scale for the axes is in Bohr radii (atomic units). The values on the dashed line and the short dashed line show corresponding probability density contours.

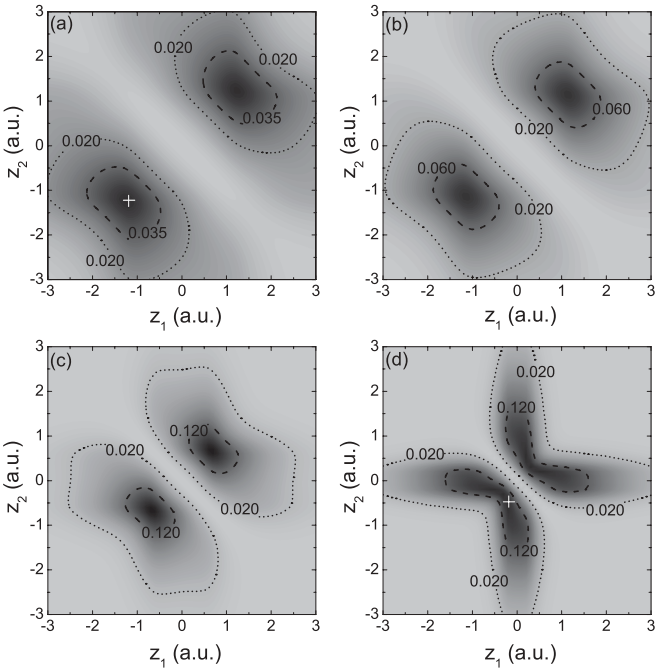

FIG. 4. The z_1-z_2 probability density distribution of the lowest $^1\Sigma_u$ state at equilibrium distance for specific field strength. (a) $\gamma = 0.0$ a.u., $R = 2.43$ a.u.; (b) $\gamma = 1.0$ a.u., $R = 2.3$ a.u.; (c) $\gamma = 10.0$ a.u., $R = 1.30$ a.u.; (d) $\gamma = 100.0$ a.u., $R = 0.490$ a.u. The length scale for the axes is in Bohr radii (atomic units). The values on the dashed line and the short dashed line show corresponding probability density contours. The white cross denotes the coordinates of the corresponding largest probability density.

are $(-0.5, -0.2)$, $(0.2, 0.5)$, and $(0.5, 0.2)$, respectively]. The geometry of the probability density distribution, illustrated by the contour of 0.020 (the short dashed lines in Fig. 4), changes dramatically with increasing field strength. In the strong magnetic-field case, the electrons also tend to locate near the same nucleus, but one locates between the nuclei (the Coulomb repulsion between two nuclei is reduced) and the other locates outside. In Fig. 4(d), the tails along z_1 and z_2 axis imply that the electron which tends to locate outside the nuclei could distribute in a relatively broad region along the z axis in a strong magnetic field.

IV. CONCLUSION

In this work, we study the electronic structure and properties of the hydrogen molecule for the lowest $^1\Sigma_g$ and $^1\Sigma_u$ state in parallel magnetic fields. Compared to the results calculated using the Gaussian basis set, the results we attained were closer to the best available data in the literature. In the presence of magnetic fields, the improvements in total energies are more than 6×10^{-4} a.u. and average 5×10^{-4} a.u. for the lowest $^1\Sigma_g$ and $^1\Sigma_u$ state, respectively. The z_1-z_2 probability density distributions of the two states at the corresponding equilibrium distances were calculated and analyzed. It showed that the probability of electrons locating between two nuclei increases with increasing field strength. Therefore, the equilibrium distances decrease and the dissociation energies at equilibrium distances increase. All our calculations have been carried out on a Dawning TC5000 cluster.

ACKNOWLEDGMENTS

This work was supported by the National Natural Science Foundation of China (Grants No. 11104208 and No. 10874133) and by "the Fundamental Research Funds for the Central Universities."

APPENDIX

All the integrations involving here are evaluated in Cartesian coordinates. First, we rewrite the atomic orbital in Eq. (5) as

$$\phi_i\left(r,+\frac{R}{2}\right) = \sum_{\sigma}\binom{|m_i|}{\sigma}\sum_{\tau}\binom{k_i}{\tau} \times [i\,\mathrm{sgn}(m_i)]^{\sigma} x^{|m_i|-\sigma+2(k_i-\tau)} y^{\sigma+2\tau} \times \left(z-\frac{R}{2}\right)^{l_i} e^{-\alpha_i x^2-\alpha_i y^2-\beta_i[z-(R/2)]^2}. \quad \text{(A1)}$$

The overlap matrix elements can be obtained in an analytic expression using the Gaussian-type basis. The matrix elements for the kinetic, paramagnetic, and diamagnetic terms can be reduced to simple overlap elements. In order to evaluate the matrix elements of nucleus attraction and electron repulsion, Singer transformation is used to regularize the singularities.

$$\frac{1}{f(r)} = \frac{2}{\sqrt{\pi}}\int_0^{\infty} e^{-f^2(r)u^2}du. \quad \text{(A2)}$$

For the electron-nucleus and electron-electron integrals, $f(r)$ is $1/(|r \pm R/2|)$ and $1/(|r_1 - r_2|)$, respectively. For evaluating the electron-nucleus integral, we defined an integral I:

$$I := \int_0^\infty du \int dx_1 dx_2 x_1^{n_{x_{ik}}} x_2^{n_{x_{jl}}} e^{-\alpha_{ik} x_1^2} e^{-\alpha_{ik} x_2^2} e^{-\gamma(x_2-x_1)^2} e^{-u^2 x_1^2} \int dy_1 dy_2 y_1^{n_{y_{ik}}} y_2^{n_{y_{jl}}} e^{-\alpha_{ik} y_1^2} e^{-\alpha_{ik} y_2^2} e^{-\gamma(y_2-y_1)^2} e^{-u^2 y_1^2}$$
$$\times \int dz_1 dz_2 (z_1 - D)^{n_{z_i}} (z_2 - D)^{n_{z_j}} (z_1 + D)^{n_{z_k}} (z_2 + D)^{n_{z_l}} e^{-\beta_i (z_1-D)^2} e^{-\beta_k (z_1+D)^2} e^{-\beta_j (z_2-D)^2} e^{-\beta_l (z_2+D)^2}$$
$$\times e^{-\gamma(z_2-z_1)^2} e^{-u^2 (z_1-D)^2}. \tag{A3}$$

Integrating over coordinate space, we obtained

$$I = \int_0^\infty du \sum C_{xy} (1 + a_u u^2)^{-T_{xy}} \sum C_z (1 + b_u u^2)^{-T_z} \mathrm{e}^{C_{ze}[1/(1+b_u u^2)]}, \tag{A4}$$

$$a_u = \frac{\alpha_{jl} + \gamma}{\alpha_{ik}\alpha_{jl} + \alpha_{ijkl}\gamma}, \quad b_u = \frac{\beta_{jl} + \gamma}{\beta_{ik}\beta_{jl} + \beta_{ijkl}\gamma}, \tag{A5}$$

where T_{xy} and T_z are positive integers or half-integers; C_{xy}, C_z, and C_{ze} are some finite constants. As the function including u at the exponent had the same form as the expression $1 + b_u u^2$ in the formulas, Taylor expansion was considered.

$$I = \int_0^\infty du \sum C_{xy} (1 + a_u u^2)^{-T_{xy}} \sum C_z (1 + b_u u^2)^{-T_z} \sum_k \frac{1}{k!} C_{ze}^k (1 + b_u u^2)^{-T_z - k}. \tag{A6}$$

Finally, the electron-nucleus integral is

$$I = \sum C_{xy} C_z \sum_k \frac{1}{k!} C_{ze}^k {}_2F_1\left(T_z + k, \frac{1}{2}, T_{xy} + T_z + k; \frac{a_u - b_u}{a_u}\right). \tag{A7}$$

Therefore, the electron-nucleus integral can be expressed in hypergeometric function and evaluated eventually under Taylor expansion. The electron-electron integral can also be treated the same as the electron-nucleus integral although the electron-electron integral is more complicated.

[1] J. C. Kemp, J. B. Swedlund, J. D. Landstreet, and J. R. P. Angel, Astrophys. J. **161**, L77 (1970).
[2] J. Truemper, W. Pietsch, C. Reppin, W. Voges, R. Stauber, and E. Kendziorra, Astrophys. J. **219**, L105 (1978).
[3] D. Lai, Rev. Mod. Phys. **73**, 629 (2001).
[4] V. B. Timofeev and A. V. Chernenko, Pis'ma Zh. Eksp. Teor. Fiz. **61**, 603 (1995) [JETP Lett. **61**, 617 (1995)].
[5] H. Ruder, G. Wunner, H. Hernold, F. Geyer, *Atoms in Strong Magnetic Fields* (Springer, Berlin, 1994).
[6] P. Schmelcher and W. Schweizer, *Atoms and Molecules in Strong External Fields* (Springer, Berlin, 1998).
[7] M. D. Jones, G. Ortiz, and D. M. Ceperley, Phys. Rev. E **55**, 6202 (1997).
[8] M. Braun, W. Schweizer, and H. Elster, Phys. Rev. A **57**, 3739 (1998).
[9] A. Scrinzi, Phys. Rev. A **58**, 3879 (1998).
[10] M. Hesse and D. Baye, J. Phys. B **37**, 3937 (2004).
[11] W. Becken, P. Schmelcher, and F. K. Diakonos, J. Phys. B **32**, 1557 (1999).
[12] W. Becken and P. Schmelcher, J. Phys. B **33**, 545 (2000).
[13] X. Wang, J. Zhao, and H. Qiao, Phys. Rev. A **80**, 053425 (2009).
[14] J. M. Peek and J. Katriel, Phys. Rev. A **21**, 413 (1980).
[15] V. K. Khersonskii, Sov. Astron. **31**, 646 (1987).
[16] U. Kappes and P. Schmelcher, Phys. Rev. A **51**, 4542 (1995).
[17] U. Kappes and P. Schmelcher, Phys. Rev. A **53**, 3869 (1996).
[18] U. Kappes and P. Schmelcher, Phys. Rev. A **54**, 1313 (1996).
[19] Yu. P. Kravchenko and M. A. Liberman, Phys. Rev. A **55**, 2701 (1997).
[20] P. Schmelcher, L. S. Cederbaum, and H.-D. Meyer, Phys. Rev. A **38**, 6066 (1988).
[21] X. Guan, B. Li, and K. T. Taylor, J. Phys. B **36**, 3569 (2003).
[22] M. Vincke and D. Baye, J. Phys. B **39**, 2605 (2006).
[23] D. Baye, A. Joos de ter Beerst, and J.-M. Sparenberg, J. Phys. B **42**, 225102 (2009).
[24] A. V. Turbiner and J. C. López-Vieyra, Phys. Rep. **424**, 309 (2006).
[25] T. S. Moneiro and K. T. Taylor, J. Phys. B **23**, 427 (1990).
[26] S. Basile, F. Trombetta, and G. Ferrante, Nuovo Cimento D **9**, 457 (1987).
[27] A. V. Turbiner, Pis'ma Zh. Eksp. Teor. Fiz. **38**, 510 (1983) [JETP Lett. **38**, 618 (1983)].
[28] A. V. Korolev and M. A. Liberman, Phys. Rev. A **45**, 1762 (1992).
[29] D. Lai, E. E. Salpeter, and S. L. Shapiro, Phys. Rev. A **45**, 4832 (1992).
[30] G. Ortiz, M. D. Jones, and D. M. Ceperley, Phys. Rev. A **52**, R3405 (1995).
[31] D. Lai and E. E. Salpeter, Phys. Rev. A **53**, 152 (1996).
[32] Yu. P. Kravchenko and M. A. Liberman, Phys. Rev. A **56**, R2510 (1997).

[33] T. Detmer, P. Schmelcher, F. K. Ddiakonos, and L. S. Cederbaum, Phys. Rev. A **56**, 1825 (1997).
[34] T. Detmer, P. Schmelcher, and L. S. Cederbaum, Phys. Rev. A **57**, 1767 (1998).
[35] M. Sadhukhan and B. M. Deb, J. Mol. Struct.: THEOCHEM **943**, 65 (2010).
[36] W. H. Press, S. A. Teukolsky, W. T. Vetterling, and B. P. Flannery, *Numerical Recipes in FORTRAN 77: The Art of Scientific Computing*, 2nd ed. (Cambridge University Press, Cambridge, 1997).
[37] Z.-C. Yan and G. W. F. Drake, Phys. Rev. A **52**, 3711 (1995).
[38] K. Pauchuchi, Phys. Rev. A **82**, 032509 (2010).
[39] W. Cencek, J. Komasa, and J. Rychlewski, Chem. Phys. Lett. **246**, 417 (1995).
[40] O.-A. Al-Hujaj and P. Schmelcher, Phys. Rev. A **61**, 063413 (2000).